
Journal of Electrochemistry

Li-Wen Wu, Wei Wang, Yi-Fan Huang. Electrochemical Surface-Enhanced Raman Spectroscopic Studies on Nickel Ultramicroelectrode[J]. *Journal of Electrochemistry*, 2021, 27(2): 208-215.

VOLUME 27
DOI: <https://doi.org/10.1007/s10804-021-0140-1>
Electrochemistry Celebrates 100 Years of Chemistry at Xiamen University (I)

Nickel (Ni) electrodes are widely used in electrochemical researches. Understanding electrochemical processes on Ni electrodes through *in situ* characterization of adsorbed species on their surfaces is helpful for rational optimization and application of Ni electrochemistry. Microelectrochemical surface-enhanced Raman spectroscopy (μ EC-SERS) combines the mass transfer feature of ultramicroelectrode with high-sensitivity characterizations of molecular structures, which is a powerful method for studying Ni electrochemistry on polarization and non-equilibrium conditions. The key point of performing μ EC-SERS is

Electrochemical Surface Enhanced Raman Spectroscopic Studies

Here, we demonstrate a method of preparing a SERS-active Ni ultramicroelectrode through electrochemical deposition of several atomic layers of metallic Ni onto a SERS-active gold (Au) ultramicroelectrode. Firstly, a SERS-active Au ultramicroelectrode was made through electrochemical

deposition of Au nanoparticles. A smooth polycrystalline Au ultramicroelectrode with a diameter of 10 μm was made by sealing a Au wire into a glassy tube. The Au nanoparticles of 55 nm in diameter were adsorbed from Au sol onto the Au ultramicroelectrode under an electrochemical polarization at 1.8 V. The scanning electron microscopic (SEM) images showed that Au nanoparticles aggregated on surface.

Yi-Fan Huang
On the prepared Au ultramicroelectrode adsorbed by Au nanoparticles, a thin and compact Ni layer was deposited by using galvanostatic method in 5 $\text{mmol}\cdot\text{L}^{-1}$ $\text{Ni}(\text{NO}_3)_2$ electrolyte. The thickness of Ni layer was controlled via the charge. The voltammograms of the prepared SERS-active Ni ultramicroelectrode in

0.1 $\text{mol}\cdot\text{L}^{-1}$ NaOH showed the characters of polycrystalline Ni electrode. Since the SERS activity decreased as a result of the increase in the thickness of Ni layer, the SERS measurements of 4-methylthiophenol in air were carried out for evaluating SERS activity. The comparisons in the intensity of the band at 1077 cm^{-1} from the 4-methylthiophenol adsorbed on the ultramicroelectrode made by using 10 $\mu\text{A}\cdot\text{cm}^{-2}$, 50 $\mu\text{A}\cdot\text{cm}^{-2}$, 100 $\mu\text{A}\cdot\text{cm}^{-2}$, 500 $\mu\text{A}\cdot\text{cm}^{-2}$ and 1000 $\mu\text{A}\cdot\text{cm}^{-2}$ indicated that the rate and charge of deposition are key in determining the coverage status of Ni layer and the SERS activity. An optimized SERS activity on a compact Ni was obtained by electrodepositing 5 atomic layers of Ni at a current density of 100 $\mu\text{A}\cdot\text{cm}^{-2}$.

To demonstrate the application of Ni ultramicroelectrode in the *in-situ* μ EC-SERS measurement, the molecule of 4-methylthiophenol, employed as a probe, was adsorbed onto the prepared Ni ultramicroelectrode through spontaneous adsorption in the methanol solution of 4-methylthiophenol. The obtained SERS spectra showed characteristic bands of 4-methylthiophenol. In addition, stark effect of the bands was observed, indicating the successful application of Ni ultramicroelectrode in the *in-situ* μ EC-SERS measurement.

The preparation methodology of SERS-active ultramicroelectrode enables the *in-situ* μ EC-SERS measurement on Ni under electrochemical polarization or non-equilibrium reaction conditions, which exhibits a good potential application in studying Ni electrochemistry.

Available at: <https://jelectrochem.xmu.edu.cn/journal/vol27/iss2/7>

应用镍超微电极的电化学表面 增强拉曼光谱技术研究

吴丽文¹, 王 珝², 黄逸凡^{1*}

(1. 上海科技大学物质科学与技术学院, 上海 201210; 2. 井冈山大学化学化工学院, 江西 吉安 343009)

摘要: 镍(Ni)电极在电化学中应用广泛。原位表征 Ni 电极表面的吸附物种有益于帮助理解电极反应历程、指导发展高效电催化剂。应用超微电极作为工作电极的电化学表面增强拉曼光谱技术结合了超微电极表面的传质特性和分子水平的高灵敏度表征, 是研究 Ni 电化学的有力手段。本文所述的研究工作通过在金(Au)超微电极表面电吸附具有 SERS 活性的 Au 纳米粒子并恒电流沉积金属 Ni 薄层, 制备并表征了具有 SERS 活性的 Ni 超微电极。在氢氧化钠溶液中的循环伏安实验和以 4-甲基苯硫酚分子作为探针分子的 SERS 实验结果表明, 沉积速率和沉积电量是影响超微电极表面 Ni 的覆盖度和 SERS 活性的关键因素。在吸附了直径为 55 nm Au 纳米粒子的、直径为 10 μm Au 的超微电极表面, 以 100 μA·cm⁻² 电流密度电沉积厚度约为 5 个原子层 Ni 的条件下, 可获得 Ni 覆盖完好的、具有最强 SERS 活性的 Ni 超微电极。

关键词: 镍; 超微电极; 表面增强拉曼光谱; 电沉积

1 引言

镍元素储量丰富, 价格便宜, 在电催化、电镀、电池、超级电容器等方面应用广泛^[1-7]。例如, Stamenkovic 等^[4]发现 Pt_xNi(111)的氧还原反应催化活性比 Pt(111)表面高 10 倍、比 Pt/C 催化剂高 90 倍; Yang 等^[5]发现氮掺杂石墨烯锚定的 Ni 单原子催化剂在二氧化碳还原反应中具有非常优异的催化活性及稳定性; Wang 等^[6]研究发现不同氧化程度石墨烯上生长的 Ni(OH)₂纳米晶体在充放电电流密度为 2.8 A·g⁻¹时, 比电容可达 1335 F·g⁻¹。Sun 等^[7]发现以 NiS 作为对电极的染料敏化太阳能电池的转换效率为 6.83%, 接近于以 Pt 作为对电极时的转换效率 7%。在微观尺度上理解 Ni 电极表面的电极过程将有助于理解 Ni 电极与性能之间的构效关系, 指导发展高效催化剂。

原位谱学电化学技术能够在微观尺度上提供

电化学过程的多种信息, 已成为研究电化学过程的重要手段^[8]。电化学表面增强拉曼光谱(electrochemical surface-enhanced Raman spectroscopy, EC-SERS) 技术具有灵敏度高、受水分子的影响小、能够直接提供表面物种低频振动信息等特点, 已广泛应用于研究电极/电解质界面^[9-12]。鉴于 Ni 电极的广泛应用, EC-SERS 也被应用于研究 Ni 表面的电极过程。例如, Kostecki 等^[13]利用 EC-SERS 研究了碱性 NaOH 溶液中, 多次充放电循环对 Ni(OH)₂ 薄膜结构以及组成的影响; Koper 等^[14]利用 EC-SERS 研究 NiOOH 催化剂在氧析出反应体系中的 pH 效应, 证明 pH 值对 NiOOH 表面去质子化有重要影响; Louie 等^[15]应用 EC-SERS 研究了 Ni-Fe 膜催化剂在碱性电解质中的结构与 OER 活性的关系; Li 等^[16]结合 EC-SERS 和密度泛函理论(DFT)表征了 PtNi 合金表面的氢气电化学氧化过

引用格式: Wu L W, Wang W, Huang Y F. Electrochemical surface-enhanced raman spectroscopic studies on nickel ultramicro-electrode. *J. Electrochem.*, 2021, 27(2): 208-215.

程。这些结果为理解相应的电化学过程提供了大量分子水平的细节,提升了对Ni表面电极过程的理解。由于通常的EC-SERS实验主要是在直径约为2 mm(或更大)的圆盘电极表面开展,而拉曼光谱的光斑仅为数微米,这使得电化学信号无法与SERS信号严格对应。进一步地利用EC-SERS研究Ni表面的电极过程需要严格关联电化学信息和SERS信息,特别是在研究电化学反应时,还需要考虑反应的传质问题。

基于超微电极的 μ EC-SERS技术是一种应用超微电极作为工作电极的EC-SERS技术^[17-20]。超微电极是指至少在一个维度上小于25 μm 的电极,具有尺寸小、IR降可忽略、传质快、响应快等优点^[8]。 μ EC-SERS使用直径与拉曼光谱光斑大小差别不大的超微电极,这使得拉曼光谱光斑能够尽可能多地覆盖整个电极表面,从实验上严格关联整个超微电极表面的电化学过程与SERS光谱。同时,超微电极的扩散层很薄,可以保证物种在光谱电化学实验中的传质不受影响。

由于Ni表面的SERS效应弱,为了在Ni表面开展 μ EC-SERS研究,需要探索和优化具有SERS活性的Ni超微电极的制备方法。目前,获得具有SERS活性的Ni电极(普通大电极)主要采用以下方法:1)通过电化学氧化-还原法将纯Ni电极表面粗糙^[21-23];2)在不具有SERS活性的电极上(GC、Ni等)上电沉积Ni的纳米结构^[24];3)在纯Ni电极表面沉积Ag、Au纳米结构^[13,25];4)在具有SERS活性的电极表面(Au、Ag等)上电沉积Ni^[14,26,27];5)制备具有SERS活性的Au-Core@Ni-Shell纳米粒子^[28]并滴涂在电极上。笼统而言,SERS活性主要来源于纳米结构的等离激元引起的局域光电场的巨大增强^[29,30]。现有研究结果表明,Au纳米结构具有优异的SERS活性、稳定性及可重现性。基于Au纳米结构的活性,SERS技术进一步发展,并可用于研究不具有SERS活性的体系,例如针尖增强拉曼光谱技术^[31-33]、采用核壳结构的SERS技术^[34,35]等。因此,我们选择使用在具有SERS活性的Au超微电极上电沉积Ni的方法来制备具有SERS活性的Ni超微电极。首先,通过控电极电势电吸附Au纳米粒子制备具有SERS活性的Au超微电极^[36]。由于超微电极表面的传质很快,吸附纳米粒子的方法可以有效避免因采用氧化还原方法粗糙Au超

微电极而在表面产生微腔^[18]。相较于通过滴涂法、自组装法、机械抛光法等在通常使用的大电极构建SERS活性的方法,这样的方法也更易于在超微电极上实现。然后,在具有SERS活性的Au超微电极表面恒电流沉积Ni薄层。由于SERS的光电场增强机制是一种长程效应,Ni表面的光电场得到增强。因此,这种方法制备的Ni超微电极具有SERS活性。在此基础之上,为了获得较强且稳定的SERS活性,我们还将进一步探索优化相关参数。

2 实验

2.1 试剂与仪器

高氯酸(HClO₄, Suprapur)、高氯酸钠(NaClO₄, Emsure)购自Merck公司。三氯化六氨合钌(Ru(NH₃)₆Cl₃, 98%)、氢氧化钠(NaOH, 99.99%)、硝酸镍(Ni(NO₃)₂·6H₂O, 99.999%)、4-甲基苯硫酚(C₇H₈OS, 98%)购自Sigma-Aldrich公司。氯化钾(KCl, 99.997%)购自Alfa-Aesar公司,直径为10 μm 的Au丝购自Goodfellow。实验中所用水均为Milli-Q产超纯水,电阻率18.2 M $\Omega\cdot\text{cm}$ 。

使用JEOL公司的JSM-7800F Prime型扫描电子显微镜(SEM)对纳米粒子及超微电极的形貌进行表征。采用Renishaw公司的In-Via共焦显微拉曼光谱仪进行SERS实验,激发光为He-Ne激光,其波长为632.8 nm,到达样品表面的激光功率为0.71 mW,物镜的数值孔径为0.5,放大倍数为50 \times 。电势控制及电化学实验使用Solartron公司Modulab XM型电化学工作站。

2.2 金纳米粒子制备

采用Frens法^[37]合成Au纳米粒子:将50 mL质量分数为0.01%的HAuCl₄水溶液加热至沸腾,迅速加入0.35 mL质量分数为1%柠檬酸钠水溶液;约1 min后,溶液颜色由淡黄色变成灰黑色;2 min后溶液变为棕红色;继续保持微沸40 min后自然冷却,得到棕红色粒径约为55 nm的Au纳米粒子溶胶。

2.3 金超微电极制备

采用激光拉制法制备Au超微电极^[18,38-40]。首先,将直径10 μm Au丝放置到玻璃管的中央;然后使用激光拉制仪对玻璃管加热并施加弱拉力,使玻璃管中间稍微向两端延伸以细化;接着将玻璃管两端同时与软管密封连接,再连接到真空泵对体系抽真空,对玻璃管和Au丝加热密封;最后

从玻璃管中间最细处截断后, 将 50 μm 金属 Ni 丝放置于玻璃管中与 Au 丝导通, 再使用金相砂纸打磨电极断面, 使 Au 丝暴露出来, 即制备得 Au 超微电极。

2.4 具有 SERS 活性的金超微电极制备

将 Au 微电极置于 Au 纳米粒子溶液中, 控制恒电位 1.8 V^[36], 可获得具有 SERS 活性的 Au 超微电极。

2.5 具有 SERS 活性的镍超微电极制备

利用恒电流沉积法在上述具有 SERS 活性 Au 超微电极上沉积 Ni。电解质溶液含 5 mmol·L⁻¹ Ni(NO₃)₂。电解池采用三电极体系, 工作电极为吸附纳米粒子后的 Au 超微电极, 对电极为铂片电极, 电势均相对于可逆氢电极 RHE。Ni 的厚度可根据工作电极的实际表面积及电沉积电流密度调整。沉积单层 Ni 所需电量为 726 μC·cm⁻²^[14], 则沉积层厚度和沉积时间满足如下关系:

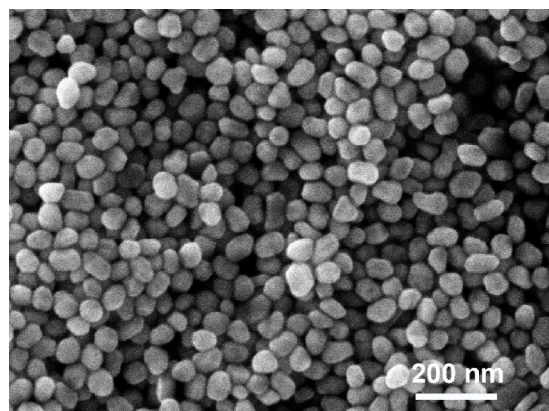


图 1 55 nm Au 纳米粒子的扫描电镜图

Figure 1 SEM image of 55 nm Au nanoparticles

$$t = \frac{d \times 726 \mu\text{C} \cdot \text{cm}^{-2}}{j}$$

t 为沉积时间, *d* 为沉积金属层数, *j* 为沉积电流

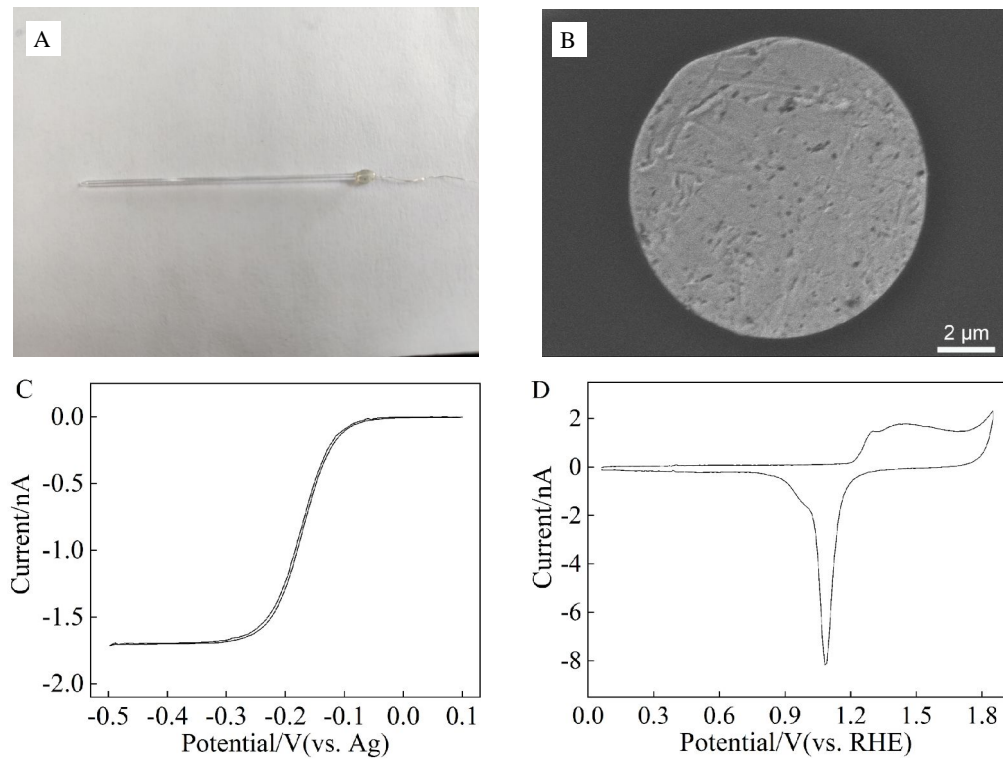


图 2 A. 直径 10 μm 的 Au 超微电极的照片; B. 直径 10 μm 的 Au 超微电极的扫描电镜图; C. Au 超微电极在 1 mmol·L⁻¹ Ru(NH₃)₆Cl₃ + 0.1 mol·L⁻¹ KCl 溶液中的循环伏安曲线, 扫速为 10 mV·s⁻¹; D. Au 超微电极在 0.1 mol·L⁻¹ HClO₄ 溶液中的循环伏安曲线, 扫速为 500 mV·s⁻¹。

Figure 2 A. Photograph of 10 μm Au ultramicroelectrode; B. SEM image of 10 μm Au ultramicroelectrode; C. Steady-state voltammogram of the Au ultramicroelectrode in 1 mmol·L⁻¹ Ru(NH₃)₆Cl₃ + 0.1 mol·L⁻¹ KCl. Scan rate: 10 mV·s⁻¹; D. Cyclic voltammogram of the Au ultramicroelectrode in 0.1 mol·L⁻¹ HClO₄. Scan rate: 500 mV·s⁻¹.

密度。

3 结果与讨论

3.1 金纳米粒子表征

我们采用 SERS 活性良好、稳定、重现性好的 Au 纳米粒子制备具有 SERS 活性的 Au 超微电极。图 1 是柠檬酸钠还原法合成的 Au 纳米粒子的 SEM 图像。从图上可看出, Au 纳米粒子表面比较光滑, 尺寸较均一, 直径约为 55 nm。

3.2 金超微电极表征

图 2A 为制备的超微电极的外观图。首先, 我们通过 SEM 表征 Au 圆盘超微电极的尺寸与表面形貌。如图 2B 所示, 该 Au 超微电极呈现规整的圆形且表面较为光滑平坦, 直径约为 10 μm。接着, 我们应用循环伏安技术表征电极的包封状态及电极表面的洁净程度。图 2C 是 Au 超微电极在 1 mmol·L⁻¹ Ru(NH₃)₆Cl₃ + 0.1 mol·L⁻¹ KCl 溶液中的稳态伏安曲线。其表现出良好的 S 型且回扫时没有产生明显的滞后, 双电层充放电电流小, 表明电极包封良好。图 2D 为 Au 超微电极在 Ar 气饱和除氧的 0.1 mol·L⁻¹ HClO₄ 溶液中的循环伏安曲线。1.3 V 开始发生含氧物种的吸附以及 1.1 V 的还原峰表明电极包封完好且表面洁净。这些表征结果说明 Au 超微电极状态良好, 将用于制备具有 SERS 活性的 Ni 超微电极。

3.3 金纳米粒子在金超微电极表面的吸附

控制电极电势可以有效地将 Au 纳米粒子吸附在普通大电极表面, 获得具有 SERS 活性的电极^[41]。图 3A 是吸附纳米粒子后的 Au 超微电极的

SEM 图, 可以明显观察到电极表面上吸附了大量 Au 纳米粒子, 且这些纳米粒子处于聚集状态。已有大量结果表明, 聚集状态下的纳米粒子能够产生耦合的等离激元, 极大地增强局域光电场, 具有良好的 SERS 活性, 甚至可达到单分子检测灵敏度^[30,42-44]。图 3B 中实线是光亮的 Au 超微电极在除氧的 0.1 mol·L⁻¹ HClO₄ 溶液中的循环伏安曲线, 虚线是吸附纳米粒子后的 Au 超微电极的循环伏安曲线。从图上可以看到, 吸附纳米粒子后的 Au 电极的氧化还原峰均明显增大, 粗糙度由 1.7 增至 8.9, 表明大量纳米粒子成功地吸附在 Au 超微电极上。这与 SEM 的表征结果相互应证。

3.4 镍超微电极的电化学及 SERS 表征

图 4A 中实线是 Au 超微电极在 Ar 气饱和除氧的 0.1 mol·L⁻¹ NaOH 中的循环伏安曲线, 虚线是以 100 μA·cm² 的电流密度在 Au 纳米粒子上沉积 Ni 后在同样的 0.1 mol·L⁻¹ NaOH 中的循环伏安曲线, 在 1.15 V 至 1.45 V 区间出现 Ni(II)/Ni(III) 的氧化还原峰, 与文献报道一致^[14,15]。观察到沉积 Ni 层的 Au 超微电极已表现出与纯 Ni 金属电极相同的伏安行为, 且没有 Au 基底的特征峰, 说明 Ni 层已将 Au 基底完全覆盖。图 4B 是电沉积形成的 Ni 超微电极的 SEM 图。

为了验证并优化 Ni 超微电极的 SERS 活性, 我们以 4-甲基苯硫酚为探针分子, 比较了以不同电流密度沉积获得的 Ni 超微电极的 SERS 活性。如图 5A 所示, 在这些 Ni 超微电极上均能够获得 4-甲基苯硫酚分子的 SERS 信号。以频率为 1077 cm⁻¹

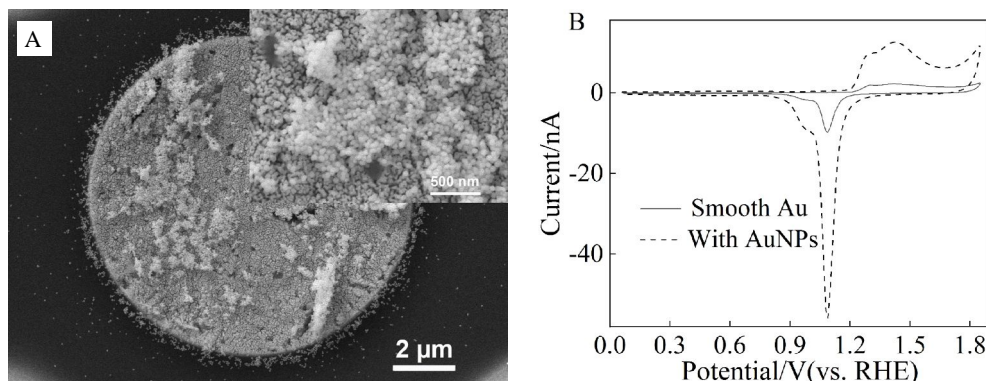


图 3 A. 吸附 Au 纳米粒子的 Au 超微电极的扫描电镜图; B. Au 超微电极吸附纳米粒子前/后在 0.1 mol·L⁻¹ HClO₄ 溶液中的循环伏安曲线, 扫速为 500 mV·s⁻¹。

Figure 3 A. SEM image of Au ultramicroelectrode with Au NPs; B. Cyclic voltammograms of smooth Au ultramicroelectrode (the solid line) and with NPs (the dashed line) in 0.1 mol·L⁻¹ HClO₄. Scan rate: 500 mV·s⁻¹.

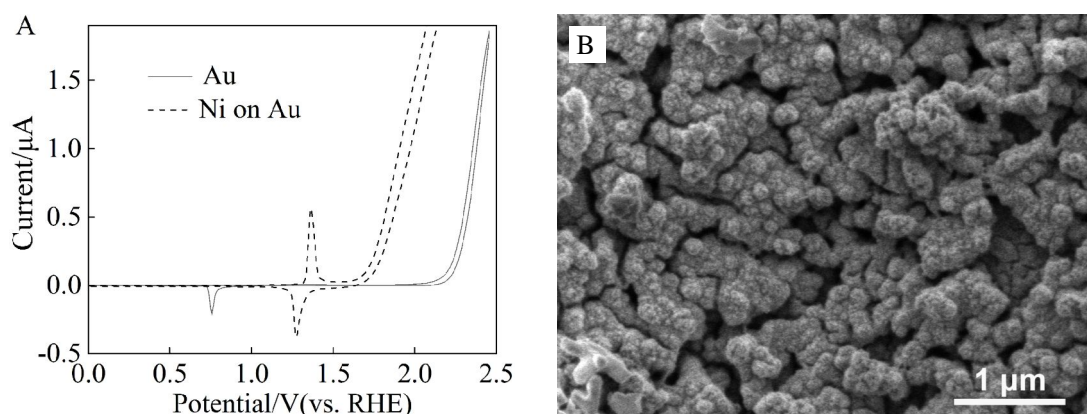


图 4 A. 沉积了 Ni 的 Au 超微电极在 $0.1 \text{ mol}\cdot\text{L}^{-1}$ NaOH 中的循环伏安曲线, 扫速为 $500 \text{ mV}\cdot\text{s}^{-1}$; B. 沉积了 Ni 的 Au 超微电极的 SEM 图。

Figure 4 A. Cyclic voltammograms of Au ultramicroelectrode (the solid line) and covered by Ni (the dashed line) in $0.1 \text{ mol}\cdot\text{L}^{-1}$ NaOH. Scan rate: $500 \text{ mV}\cdot\text{s}^{-1}$; B. SEM image of Au ultramicroelectrode covered by Ni.

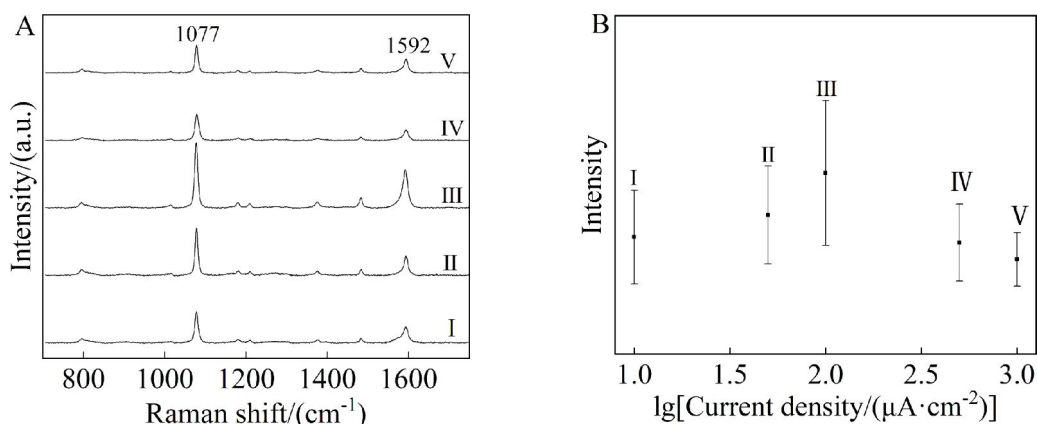


图 5 A. 4-甲基苯硫酚吸附在以不同电流密度沉积形成的 Ni 超微电极上的 SERS 谱图: I. $10 \mu\text{A}\cdot\text{cm}^{-2}$, II. $50 \mu\text{A}\cdot\text{cm}^{-2}$, III. $100 \mu\text{A}\cdot\text{cm}^{-2}$, IV. $500 \mu\text{A}\cdot\text{cm}^{-2}$, V. $1000 \mu\text{A}\cdot\text{cm}^{-2}$; B. 电沉积电流密度与 1077 cm^{-1} 强度关系图。

Figure 5 A. SERS of p-methylthiophenol adsorbed on Ni ultramicroelectrode electrodeposited by different current densities: I. $10 \mu\text{A}\cdot\text{cm}^{-2}$, II. $50 \mu\text{A}\cdot\text{cm}^{-2}$, III. $100 \mu\text{A}\cdot\text{cm}^{-2}$, IV. $500 \mu\text{A}\cdot\text{cm}^{-2}$, V. $1000 \mu\text{A}\cdot\text{cm}^{-2}$; B. Influence of electrodeposition current density on signal intensity at 1077 cm^{-1} .

的谱峰的积分强度对电沉积 Ni 时采用的电流密度作图,如图 5B 所示。当电流密度从 $10 \mu\text{A}\cdot\text{cm}^{-2}$ 增加到 $100 \mu\text{A}\cdot\text{cm}^{-2}$, SERS 信号逐渐增强;当电流密度继续增加至 $1000 \mu\text{A}\cdot\text{cm}^{-2}$, SERS 谱峰的强度减弱,这表明电沉积电流密度为 $100 \mu\text{A}\cdot\text{cm}^{-2}$ 时,电沉积产生的 Ni 超微电极具有优化的 SERS 信号。

为了验证 Ni 超微电极应用于 μ EC-SERS 研究的可行性,我们在 $0.1 \text{ mol}\cdot\text{L}^{-1}$ NaOH 溶液中采用恒电势模式测量了不同电势下吸附在 Ni 超微电极表面的 4-甲基苯硫酚的 EC-SERS 光谱。如图 6A 所示,EC-SERS 光谱随着电位改变发生了变

化。以 1077 cm^{-1} 峰为例,当电极电势从 -0.15 V 正移至 1.05 V 时,该谱峰的强度减弱且频率略微红移,这表明该 Ni 超微电极具有很好的增强活性,可用于电化学界面过程的 EC-SERS 研究。

4 结 论

通过在吸附了 Au 纳米粒子的 Au 超微电极上电化学沉积金属 Ni 薄层,我们制备了具有 SERS 活性的 Ni 超微电极。同时,根据吸附在该电极表面的 4-甲基苯硫酚分子的 SERS 光谱强度,优化了沉积 Ni 时采用的电流密度。结果表明,在吸附了 55 nm Au 纳米粒子的 $10 \mu\text{m}$ Au 超微电极表面

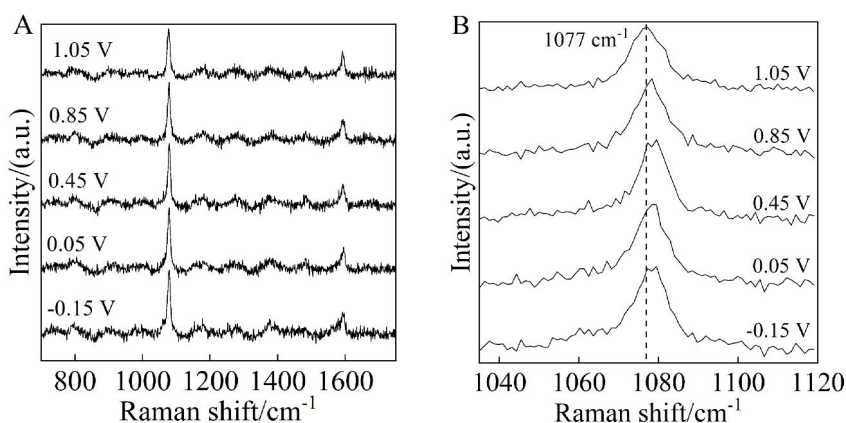


图 6 A. 吸附 4-甲基苯硫酚的 Ni 超微电极在 0.1 mol·L⁻¹ NaOH 溶液中不同电位时的 SERS 谱图;B. 不同电极电势下频率为 1077 cm⁻¹ 的 SERS 峰。

Figure 6 A. Potential dependent SERS of p-methylthiophenol adsorbed on Ni ultramicroelectrode in 0.1 mol·L⁻¹ NaOH;B. Potential dependent SERS of the peak at 1077 cm⁻¹.

使用电流密度为 100 μA·cm⁻² 进行电沉积所获得的 Ni 超微电极具有最强 SERS 活性。μEC-SERS 实验结果表明该 Ni 超微电极具有较好的 SERS 活性,未来可应用于 Ni 电极电化学的原位表征。

参考文献(References):

- [1] Ni W Y, Krammer A, Hsu C S, Chen H M, Schuler A, Hu X L. Ni₃N as an active hydrogen oxidation reaction catalyst in alkaline medium[J]. Angew. Chem. In. Ed., 2019, 58(22): 7445-7449.
- [2] Lu X F, Yu L, Lou X W. Highly crystalline Ni-doped FeP/carbon hollow nanorods as all-pH efficient and durable hydrogen evolving electrocatalysts[J]. Sci. Adv., 2019, 5(2): eaav6009.
- [3] Wang Q, Huang X, Zhao Z L, Wang M Y, Xiang B, Li J, Feng Z X, Xu H, Gu M. Ultrahigh-loading of Ir single atoms on NiO matrix to dramatically enhance oxygen evolution reaction[J]. J. Am. Chem. Soc., 2020, 142(16): 7425-7433.
- [4] Stamenkovic V R, Fowler B, Mun B S, Wang G F, Ross P N, Lucas C A, Markovic N M. Improved oxygen reduction activity on Pt₃Ni(111) via increased surface site availability[J]. Science, 2007, 315(5811): 493-497.
- [5] Yang H B, Hung S F, Liu S, Yuan K D, Miao S, Zhang L P, Huang X, Wang H Y, Cai W Z, Chen R, Gao J J, Yang X F, Chen W, Huang Y Q, Chen H M, Li C M, Zhang T, Liu B. Atomically dispersed Ni(I) as the active site for electrochemical CO₂ reduction [J]. Nat. Energy, 2018, 3(2): 140-147.
- [6] Wang H L, Casalongue H S, Liang Y Y, Dai H J. Ni(OH)₂ nanoplates grown on graphene as advanced electrochemical pseudocapacitor materials[J]. J. Am. Chem. Soc., 2010, 132(21): 7472-7477.
- [7] Sun H C, Qin D, Huang S Q, Guo X Z, Li D M, Luo Y H, Meng Q B. Dye-sensitized solar cells with NiS counter electrodes electrodeposited by a potential reversal technique[J]. Energy Environ. Sci., 2011, 4(8): 2630-2637.
- [8] Bard A J, Faulkner L R. Electrochemical methods: fundamentals and applications[M]. New York: John Wiley & Sons, Inc., 2001: 168-176.
- [9] Fleischmann M, Hendra P J, McQuillan A J. Raman spectra of pyridine adsorbed at a silver electrode[J]. Chem. Phys. Lett., 1974, 26(2): 163-166.
- [10] Albrecht M G, Creighton J A. Anomalously intense Raman spectra of pyridine at a silver electrode[J]. J. Am. Chem. Soc., 1977, 99(15): 5215-5217.
- [11] Jeanmaire D L, Van Duyne R P. Surface raman spectroelectrochemistry: Part I. Heterocyclic, aromatic, and aliphatic amines adsorbed on the anodized silver electrode[J]. J. Electroanal. Chem., 1977, 84(1): 1-20.
- [12] Wu D Y, Li J F, Ren B, Tian Z Q. Electrochemical surface-enhanced Raman spectroscopy of nanostructures[J]. Chem. Soc. Rev., 2008, 37(5): 1025-1041.
- [13] Kostecki R, McLarnon F. Electrochemical and *in situ* Raman spectroscopic characterization of nickel hydroxide electrodes: I. Pure nickel hydroxide[J]. J. Electrochem. Soc., 1997, 144: 485-493.
- [14] Diaz-Morales O, Ferrus-Suspedra D, Koper M T M. The importance of nickel oxyhydroxide deprotonation on

- its activity towards electrochemical water oxidation [J]. *Chem. Sci.*, 2016, 7(4): 2639-2645.
- [15] Louie M W, Bell A T. An investigation of thin-film Ni-Fe oxide catalysts for the electrochemical evolution of oxygen[J]. *J. Am. Chem. Soc.*, 2013, 135(33): 12329-12337.
- [16] Wang Y H, Wang X T, Ze H, Zhang X G, Radjenovic P M, Zhang Y J, Dong J C, Tian Z Q, Li J F. Spectroscopic verification of adsorbed hydroxyl intermediate in the bi-functional mechanism of hydrogen oxidation reaction[J]. *Angew. Chem. Int. Ed.*, 2021, 60(11): 5708-5711.
- [17] Kim B J, Lee D J, Kim Y R, Lim S Y, Bae J H, Kim K B, Chung T D. Gold microshell tip for *in situ* electrochemical Raman spectroscopy[J]. *Adv. Mater.*, 2012, 24(3): 421-424.
- [18] Wang W, Huang Y F, Liu D Y, Wang F F, Tian Z Q, Zhan D P. Electrochemically roughened gold microelectrode for surface-enhanced Raman spectroscopy[J]. *J. Electroanal. Chem.*, 2016, 779: 126-130.
- [19] Huang Y F, Wang W, Guo H Y, Zhan C, Duan S, Zhan D P, Wu D Y, Ren B, Tian Z Q. Microphotoelectrochemical surface-enhanced Raman spectroscopy: toward bridging hot-electron transfer with a molecular reaction[J]. *J. Am. Chem. Soc.*, 2020, 142(18): 8483-8489.
- [20] Liu N Y, Wu L W, Huang Y F. *In-situ* electrochemical Raman spectroscopy on ultramicroelectrodes[J]. *Sci. Sin. Chim.*, 2021, 51(3): 256-263.
- [21] Ren B, Huang Q J, Cai W B, Mao B W, Liu F M, Tian Z Q. Surface Raman spectra of pyridine and hydrogen on bare platinum and nickel electrodes[J]. *J. Electroanal. Chem.*, 1996, 415(1-2): 175-178.
- [22] Huang Q J, Yao J L, Mao B W, Gu R A, Tian Z Q. Surface Raman spectroscopic studies of pyrazine adsorbed onto nickel electrodes[J]. *Chem. Phys. Lett.*, 1997, 271(1-3): 101-106.
- [23] Tian Z Q, Ren B, Wu D Y. Surface-enhanced Raman scattering: from noble to transition metals and from rough surfaces to ordered nanostructures[J]. *J. Phys. Chem. B*, 2002, 106(37): 9463-9483.
- [24] Gao J S(高劲松), Ren B(任斌), Huang Q J(黄群健), Tian Z Q(田中群). Surface Raman spectra obtained from various electrodeposited transition metals[J]. *J. Electrochem.(电化学)*, 1996, 2(3): 258-261.
- [25] Xia Y Y, Wu Y W, Wu L W, Wang T Y Y, Hang T, Huang Y F, Li M. Two-step electrodeposited 3D Ni nanocone supported Au nanoball arrays as SERS substrate[J]. *J. Electrochem. Soc.*, 2020, 167(14): 142502.
- [26] Fleischmann M, Tian Z Q, Li L J. Raman spectroscopy of adsorbates on thin film electrodes deposited on silver substrates[J]. *J. Electroanal. Chem.*, 1987, 217(2): 397-410.
- [27] Fleischmann M, Tian Z Q. The induction of SERS on smooth Ag by the deposition of Ni and Co[J]. *J. Electroanal. Chem.*, 1987, 217(2): 411-416.
- [28] Bao F, Li J F, Ren B, Yao J L, Gu R A, Tian Z Q. Synthesis and characterization of Au@Co and Au@Ni core-shell nanoparticles and their applications in surface-enhanced Raman spectroscopy[J]. *J. Phys. Chem. C*, 2008, 112(2): 345-350.
- [29] Moskovits M. Surface-enhanced spectroscopy[J]. *Rev. Mod. Phys.*, 1985, 57(3): 783-826.
- [30] Willets K A, Van Duyne R P. Localized surface plasmon resonance spectroscopy and sensing[M]. *Annual Review of Physical Chemistry*, 2007, 58: 267-297.
- [31] Hayazawa N, Inouye Y, Sekkat Z, Kawata S. Metallized tip amplification of near-field Raman scattering[J]. *Opt. Commun.*, 2000, 183(1-4): 333-336.
- [32] Stöckle R M, Suh Y D, Deckert V, Zenobi R. Nanoscale chemical analysis by tip-enhanced Raman spectroscopy [J]. *Chem. Phys. Lett.*, 2000, 318(1-3): 131-136.
- [33] Pettinger B, Ren B, Picardi G, Schuster R, Ertl G. Nanoscale probing of adsorbed species by tip-enhanced Raman spectroscopy[J]. *Phys. Rev. Lett.*, 2004, 92(9): 096101.
- [34] Tian Z Q, Ren B, Li J F, Yang Z L. Expanding generality of surface-enhanced Raman spectroscopy with borrowing SERS activity strategy[J]. *Chem. Commun.*, 2007: 3514-3534.
- [35] Li J F, Zhang Y J, Ding S Y, Panneerselvam R, Tian Z Q. Core-shell nanoparticle-enhanced Raman spectroscopy [J]. *Chem. Rev.*, 2017, 117(7): 5002-5069.
- [36] Montelongo Y, Sikdar D, Ma Y, McIntosh A J S, Velleman L, Kucernak A R, Edel J B, Kornyshev A A. Electrotunable nanoplasmonic liquid mirror[J]. *Nat. Mater.*, 2017, 16(11): 1127-1135.
- [37] Frens G. Controlled nucleation for the regulation of the particle size in monodisperse gold suspensions[J]. *Nature Phys. Sci.*, 1973, 241(105): 20-22.
- [38] Shao Y, Mirkin M V, Fish G, Kokotov S, Palanker D, Lewis A. Nanometer-sized electrochemical sensors[J]. *Anal. Chem.*, 1997, 69(8): 1627-1634.
- [39] Sun P, Mirkin M V. Kinetics of electron-transfer reactions at nanoelectrodes[J]. *Anal. Chem.*, 2006, 78(18): 6526-6534.
- [40] Zhan D, Velmurugan J, Mirkin M V. Adsorption/desorption of hydrogen on Pt nanoelectrodes: evidence of surface diffusion and spillover[J]. *J. Am. Chem. Soc.*, 2009, 131(41): 14756-14760.
- [41] Ma Y, Sikdar D, Fedosyuk A, Ma Y, Sikdar D, Fedosyuk A, Velleman L, Klemme D J, Oh S H, Kucernak ARJ,

- Kornyshev A A, Edel J B. Electrotunable nanoplasmonics for amplified surface enhanced Raman spectroscopy [J]. ACS Nano, 2020, 14(1): 328-336.
- [42] Nie S, Emory S R. Probing single molecules and single nanoparticles by surface-enhanced Raman scattering [J]. Science, 1997, 275(5303): 1102-1106.
- [43] Kneipp K, Wang Y, Kneipp H, Perelman, L T, Itzkan I, Dasari R, Feld M S. Single molecule detection using surface-enhanced Raman scattering (SERS)[J]. Physical Review Letters, 1997, 78(9): 1667-1670.
- [44] Xu H X, Aizpurua J, Käll M, Apell P. Electromagnetic contributions to single-molecule sensitivity in surface-enhanced Raman scattering[J]. Phys. Rev. E, 2000, 62(3): 4318-4324.

Electrochemical Surface-Enhanced Raman Spectroscopic Studies on Nickel Ultramicroelectrode

Li-Wen Wu¹, Wei Wang², Yi-Fan Huang^{1*}

(1. School of Physical Science and Technology, ShanghaiTech University, Shanghai 201210, China;

2. College of Chemistry and Chemical Engineering, Jinggangshan University, Ji'an 343009, Jiangxi, China)

Abstract: Nickel (Ni) electrodes are widely used in electrochemical researches. Understanding electrochemical processes on Ni electrodes through *in-situ* characterization of adsorbed species on their surfaces is helpful for rational optimization and application of Ni electrochemistry. Microelectrochemical surface-enhanced Raman spectroscopy (μ EC-SERS) combines the mass transfer feature of ultramicroelectrode with high-sensitivity characterizations of molecular structures, which is a powerful method for studying Ni electrochemistry on polarization and non-equilibrium conditions. The key point of performing μ EC-SERS is to make a SERS-active Ni ultramicroelectrode.

Here, we demonstrate a method of preparing a SERS-active Ni ultramicroelectrode through electrochemical deposition of several atomic layers of metallic Ni onto a SERS-active gold (Au) ultramicroelectrode. Firstly, a SERS-active Au ultramicroelectrode was made through electrochemical adsorption of Au nanoparticles. A smooth polycrystalline Au ultramicroelectrode with a diameter of 10 μ m was made by sealing a Au wire into a glassy tube. The Au nanoparticles of 55 nm in diameter were adsorbed from Au sol onto the Au ultramicroelectrode under an electrochemical polarization at 1.8 V. The scanning electron microscopic (SEM) images showed that Au nanoparticles aggregated on surface.

On the prepared Au ultramicroelectrode adsorbed by Au nanoparticles, a thin and compact Ni layer was deposited by using galvanostatic method in 5 mmol·L⁻¹ Ni(NO₃)₂ electrolyte. The thickness of Ni layer was controlled via the charge. The voltammograms of the prepared SERS-active Ni ultramicroelectrode in 0.1 mol·L⁻¹ NaOH showed the characters of polycrystalline Ni electrode. Since the SERS activity decreased as a result of the increase in the thickness of Ni layer, the SERS measurements of 4-methylthiophenol in air were carried out for evaluating SERS activity. The comparisons in the intensity of the band at 1077 cm⁻¹ from the 4-methylthiophenol adsorbed on the ultramicroelectrode made by using 10 μ A·cm⁻², 50 μ A·cm⁻², 100 μ A·cm⁻², 500 μ A·cm⁻² and 1000 μ A·cm⁻² indicated that the rate and charge of deposition are key in determining the coverage status of Ni layer and the SERS activity. An optimized SERS activity on a compact Ni was obtained by electrodepositing 5 atomic layers of Ni at a current density of 100 μ A·cm⁻².

To demonstrate the application of Ni ultramicroelectrode in the *in-situ* μ EC-SERS measurement, the molecule of 4-methylthiophenol, employed as a probe, was adsorbed onto the prepared Ni ultramicroelectrode through spontaneous adsorption in the methanol solution of 4-methylthiophenol. The obtained SERS spectra showed characteristic bands of 4-methylthiophenol. In addition, stark effect of the bands was observed, indicating the successful application of Ni ultramicroelectrode in the *in-situ* μ EC-SERS measurement.

The preparation methodology of SERS-active ultramicroelectrode enables the *in-situ* μ EC-SERS measurement on Ni under electrochemical polarization or non-equilibrium reaction conditions, which exhibits a good potential application in studying Ni electrochemistry.

Key words: nickel; ultramicroelectrode; surface-enhanced Raman spectroscopy; electrochemical deposition